

## 2 Curvature of the Spine: Hydrostatic Pressure as an Indicator of Scoliosis

John Billingham, Birmingham; Chris Breward & Peter Howell, Oxford.

### 2.1 Introduction

Scoliosis refers to an abnormal lateral curvature of the spine. It affects between 0.5 and 2% of the population and is more common in females, usually becoming apparent during the adolescent growth spurt. The exact causes of scoliosis are unknown at present. The purpose of the present study is to investigate a currently popular hypothesis that it arises from systematic asymmetric loading of the spine and thus of the intervertebral discs. This may lead, it is thought, to permanent remodelling of the discs so that they assume a “wedge” shape. This asymmetric reshaping plays an important role in the progression and permanence of the disorder.

The intervertebral discs form the joints that allow bending of the spine. They also act as shock absorbers and help to support the loads applied by muscles and ligaments as well as weight of the head. Each disc consists of two distinct regions. The *annulus fibrosus* is composed of fibrous lamellae, made up of bundles of collagen fibres, which form “onion-like” rings around the outside of the disc, The *nucleus pulposus* is a highly hydrated gel contained inside these rings. The whole disc is composed mostly of water which, along with proteoglycans and collagen, comprises 90–95% of the tissue. The proteoglycans’ role is to generate an osmotic pressure that draws water into the disc and holds it there.

A pressure transducer has been used to measure the pressures inside intervertebral discs. In fact, by rotating the transducer, it is possible to measure the normal stresses in two perpendicular directions. In a healthy disc, the pressure is found to be roughly uniform across the disc, except in narrow regions near the edge where it drops rapidly to zero, as indicated in figure 1(a). The solid and dotted lines in this figure indicate that the pressure measured is generally independent of the orientation of the transducer. This uniformity of the pressure is found to hold even when an asymmetric load is applied. In a damaged disc, however, the pressure is found to be less isotropic and to vary more across the disc, as shown schematically in figure 1(b).

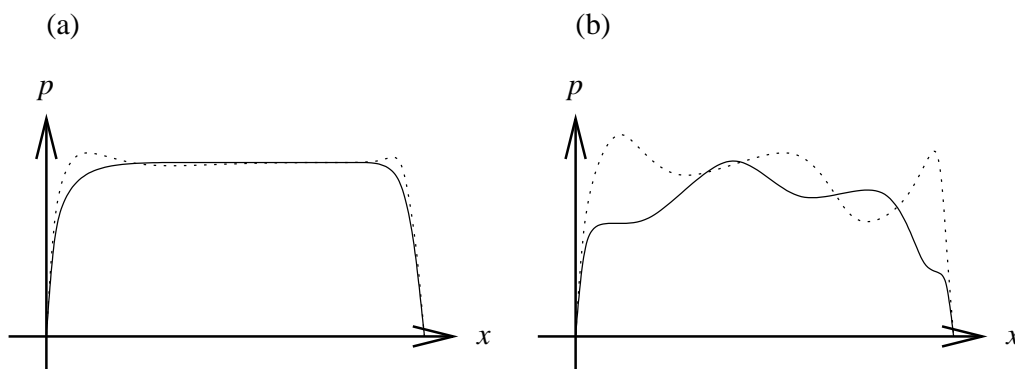


Figure 1: Typical measurements of pressure  $p$  versus distance  $x$  across an intervertebral disc; (a) healthy disc, (b) damaged disc. The solid and dotted lines indicate the pressures measured in two perpendicular directions.

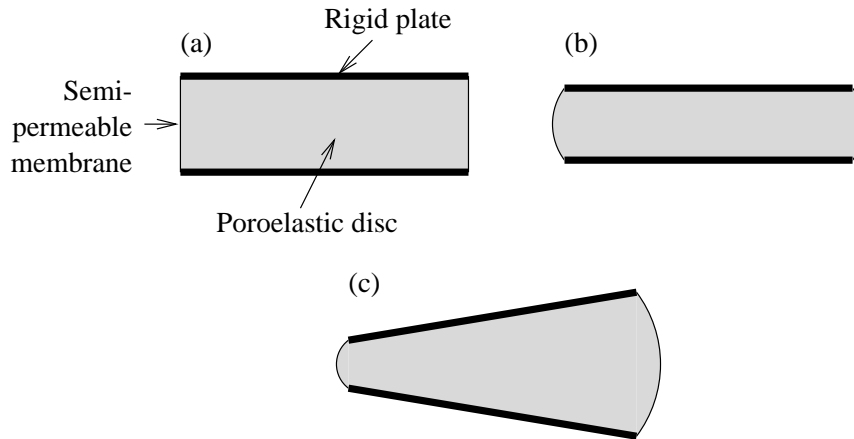


Figure 2: Schematic of a poroelastic disc.

The uniform, isotropic stress sketched in figure 1(a) suggests that any applied force is ideally supported mainly by the fluid held inside the disc. A nonuniform, anisotropic stress like that shown in figure 1(b) is more consistent with an elastic response, and probably means that the solid matrix of the disc is experiencing a significant portion of the load. Presumably, remodelling and/or damage result if the stress applied to the tissue, rather than to the liquid trapped inside it, becomes too great.

We propose to develop a mathematical model for an intervertebral disc by treating it as a poroelastic matrix that is saturated with a viscous liquid. The osmotic pressure due to the presence of proteoglycans is introduced as a pressure difference between the solid and liquid phases. Our model will determine the motion of the porous elastic matrix and the transport of fluid through it as the disc is deformed under an applied load. It will also predict the distribution of stress between the two phases, and how this depends on the material properties of each. Our eventual aim is to build in the gradual evolution of those properties as the tissue remodels under the stresses applied to it. Of particular interest is the possibility of a feedback loop, whereby remodelling acts to enhance any initial asymmetry in the system.

In this report, we limit our attention to a uniform, isotropic deformable porous medium, and only consider small deformations, so that the solid phase may be described using the classical theory of linear elasticity. We begin, however, by presenting the equations in some generality, so that nonuniformity, anisotropy and nonlinearity may all be introduced in further refinements.

## 2.2 Model for a poroelastic disc

### 2.2.1 Model description

We model the intervertebral disc as consisting of a poroelastic material that is saturated with fluid. The vertebrae are modelled by rigid plates attached to the top and bottom of the disc, as shown in figure 2(a), while stress-free boundary conditions are applied at the curved edges. The disc is assumed to be enclosed by membranes that are semi-permeable to the fluid. Since fluid may also leak into the porous vertebrae, the rigid plates are likewise treated as semi-permeable.

Now, if an axial force (*e.g.* the weight of the head) is applied to the disc, we can

expect it to deform as shown in figure 2(b). The load is supported both by the pressure in the trapped fluid and by elastic stress in the poroelastic matrix. Over time, the liquid is gradually squeezed out through the semi-permeable boundaries; this is manifested in a noticeable decrease in a person's height over the course of each day. The elastic component of stress must therefore gradually increase. Our aim is to quantify this distribution of stress between the fluid and elastic components, the idea being that excessive elastic stress may lead to damage and consequent weakening of the matrix.

Of particular interest is the possibility of a bending moment being applied to the spine, resulting in a deformation like that shown in figure 2(c). In this case, we wish to determine the asymmetry in the stress field caused in the disc. Our hypothesis is that this might lead to a gradual weakening of one side of the disc and thus make it still more susceptible to bending under everyday loads.

### 2.2.2 Governing equations

Both the solid material comprising the porous matrix and the fluid occupying the pores are assumed to be incompressible. Conservation of mass for each phase therefore implies the two equations

$$\phi_t + \nabla \cdot (\phi \mathbf{q}_\ell) = 0, \quad (2.1)$$

$$(1 - \phi)_t + \nabla \cdot \{(1 - \phi) \mathbf{q}_s\} = 0, \quad (2.2)$$

where  $\phi$  is the fluid volume fraction or porosity, while  $\mathbf{q}_\ell$  and  $\mathbf{q}_s$  are the velocities of the fluid and solid phases respectively.

Next we impose conservation of momentum for each phase, assuming that, over the timescales of interest (typically a few hours), inertia may be neglected. The only liquid stress considered is an isotropic pressure  $p_\ell$ . Thus macroscopic viscous effects are ignored, although viscosity plays a role in the pore-scale inter-phase drag  $\mathbf{D}$ . The porous matrix is characterised by an elastic stress stress tensor  $\boldsymbol{\tau}$  as well as an isotropic pressure  $p_s$  (associated with the assumed incompressibility of the solid phase). These assumptions give rise to the equations

$$\phi \nabla p_\ell = \mathbf{D}, \quad (2.3)$$

$$(1 - \phi) \nabla p_s = \nabla \cdot \boldsymbol{\tau} - \mathbf{D}. \quad (2.4)$$

Note that the stress  $\boldsymbol{\tau}$  is measured per unit area occupied by both phases; in other words it is the stress tensor that would be measured in the matrix as a whole if no liquid were present.

To close the equations, we need to impose some constitutive laws. For the interphase drag we assume that the fluid flow relative to the solid matrix satisfies Darcy's law:

$$\mathbf{K}(\phi) \cdot \mathbf{D} = \mu_\ell \phi (\mathbf{q}_s - \mathbf{q}_\ell), \quad (2.5)$$

where  $\mu_\ell$  is the fluid viscosity and  $\mathbf{K}(\phi)$  is the permeability tensor. In relating the two pressures  $p_\ell$  and  $p_s$ , we incorporate the osmotic pressure  $\pi$ , due to the presence of proteoglycans, as an interphase pressure difference. Since the proteoglycans are assumed to be attached to the incompressible solid matrix, their concentration, and hence the osmotic pressure, is a decreasing function of the porosity  $\phi$ :

$$p_s - p_\ell = \pi(\phi), \quad \pi'(\phi) < 0. \quad (2.6)$$

Finally, we need a constitutive relation between the stress tensor  $\boldsymbol{\tau}$  and the displacement field  $\mathbf{u}$ , given in terms of the velocity  $\mathbf{q}_s$  by the kinematic condition

$$\mathbf{u}_t + (\mathbf{q}_s \cdot \nabla)\mathbf{u} = \mathbf{q}_s. \quad (2.7)$$

In practice, the solid matrix is certainly anisotropic and probably experiences strains of order unity as the disc is compressed by a significant fraction of its initial thickness. A fully nonlinear anisotropic elasticity formulation would clearly lead to an extremely complicated model, which would require a difficult and time-consuming numerical solution. Furthermore, we do not at present have enough detailed information about the rheology of the disc constituents to be able to identify the many physical parameters in such a model.

In this report we use isotropic infinitesimal elasticity theory to describe the solid matrix. This both leads to a relatively tractable elastic problem and allows us to linearise the other governing equations (2.1–2.7), as described below in §2.2.3. While not particularly realistic, these simplifications result in a compact model from which we can quickly draw useful qualitative conclusions. Another approach that incorporates anisotropy in a pragmatic way and may be relevant is to assume that the solid deformation is unidirectional, as in [1].

The governing equations (2.1–2.6) are further simplified as follows. The liquid velocity  $\mathbf{q}_\ell$  and solid pressure  $p_s$  may be eliminated using (2.5) and (2.6) respectively. Then, by adding (2.1) to (2.2) and (2.3) to (2.4), we obtain two equations representing net conservation of mass and momentum for the two-phase continuum as a whole, namely

$$\nabla \cdot \left( \mathbf{q}_s - \frac{\phi}{\mu_\ell} \mathbf{K}(\phi) \cdot \nabla p_\ell \right) = 0, \quad (2.8)$$

and

$$\nabla \cdot \boldsymbol{\tau} = \nabla p_\ell + (1 - \phi)\nabla\pi(\phi). \quad (2.9)$$

Along with (2.2), or

$$\phi_t = \nabla \cdot \{(1 - \phi)\mathbf{q}_s\}, \quad (2.10)$$

this comprises a closed system for  $\phi$ ,  $\mathbf{q}_s$  and  $p_\ell$ , once  $\boldsymbol{\tau}$  has been constituted.

### 2.2.3 The linearised isotropic problem

Now we simplify the equations derived heretofore by treating the solid phase as isotropic and assuming that the displacement is small enough for infinitesimal elasticity theory to apply. Thus the solid stress tensor takes the form

$$\tau_{ij} = \lambda(\nabla \cdot \mathbf{u})\delta_{ij} + \mu \left( \frac{\partial u_i}{\partial x_j} + \frac{\partial u_j}{\partial x_i} \right), \quad (2.11)$$

where  $\lambda$  and  $\mu$  are the Lamé constants (for the whole matrix, recall, not just the solid phase). It is consistent with (2.11) to assume that  $\phi$  varies only slightly from its initial value  $\phi_0$  (assumed uniform):

$$\phi = \phi_0 + \tilde{\phi}, \quad \left| \tilde{\phi} \right| \ll 1. \quad (2.12)$$

If the solid matrix is isotropic, then the permeability tensor takes the form  $\mathbf{K} = k(\phi)\mathbf{I}$ , where  $\mathbf{I}$  is the identity, *i.e.* to leading order,

$$\mathbf{K} \sim k(\phi_0)\mathbf{I}. \quad (2.13)$$

In the infinitesimal theory, the kinematic condition (2.7) reduces to

$$\mathbf{u}_t \sim \mathbf{q}_s, \quad (2.14)$$

while the osmotic pressure is approximated by

$$\pi \sim \pi(\phi_0) + \pi'(\phi_0)\tilde{\phi}. \quad (2.15)$$

The linearised version of (2.10) may be integrated with respect to  $t$ , assuming that  $\mathbf{u}$  and  $\tilde{\phi}$  are both zero initially, to obtain

$$\tilde{\phi} = (1 - \phi_0)\nabla \cdot \mathbf{u}. \quad (2.16)$$

The other two governing equations (2.8) and (2.9) reduce to

$$\tilde{\phi}_t = \left( \frac{\phi_0(1 - \phi_0)k(\phi_0)}{\mu_\ell} \right) \nabla^2 p_\ell, \quad (2.17)$$

$$(\lambda + \mu)\nabla(\nabla \cdot \mathbf{u}) + \mu\nabla^2 \mathbf{u} = \nabla p_\ell + (1 - \phi_0)\pi'(\phi_0)\nabla\tilde{\phi}. \quad (2.18)$$

It is straightforward to eliminate  $p_\ell$  and  $\mathbf{u}$  from (2.16–2.18) to obtain a diffusion equation for  $\tilde{\phi}$ :

$$\tilde{\phi}_t = D\nabla^2\tilde{\phi}, \quad D = \frac{\phi_0 k(\phi_0)}{\mu_\ell} \{ \lambda + 2\mu - (1 - \phi_0)^2 \pi'(\phi_0) \}. \quad (2.19)$$

Although this is not particularly helpful in solving the problem, since the boundary conditions (see below) are not easily stated in terms only of  $\tilde{\phi}$ , it does give the useful insight that changes in the porosity due to displacement of the boundary diffuse through the matrix, with an effective diffusivity  $D$ . Notice that we expect  $\pi'$  to be negative, so there is no potential difficulty associated with  $D$  changing sign.

#### 2.2.4 Boundary conditions

Before any forces are applied, the poroelastic continuum is assumed to occupy a disc of radius  $L$  and thickness  $2a$ . We adopt the coordinate system  $(x, y, z)$  shown in figure 3, with the  $x$ - and  $y$ -axes in the mid-plane of the disc and the  $z$ -axis normal to that plane, so that the initial configuration is given by  $x^2 + y^2 \leq L^2$ ,  $-a \leq z \leq a$ . The situation is complicated by the fact that the curved edge of the disc is a free boundary. Since we are using infinitesimal elasticity theory, however, the displacement field is assumed to be small. It is asymptotically consistent with this approach to apply the boundary conditions on the undeformed boundary — to the order of approximation used in deriving (2.16–2.18), Eulerian and Lagrangian variables are equivalent.

As described in §2.2.1, the upper and lower surfaces of the disc are attached to rigid plates, whose displacements are assumed to be specified. We further suppose, as indicated

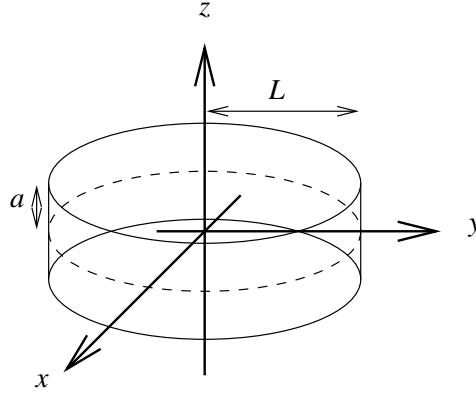


Figure 3: Definition sketch for the coordinate system  $(x, y, z)$ .

in figure 2(c), that the force/couple systems applied to the upper and lower surfaces are equal and opposite, so that symmetry in the plane  $z = 0$  is preserved. We therefore have

$$\mathbf{u} = (0, 0, \pm W) \quad \text{on} \quad z = \pm a, \quad (2.20)$$

where  $W$  is a given function of  $x$ ,  $y$  and  $t$ , typically linear in  $x$  and  $y$ .

Recall that the end plates are supposed to be semi-permeable, to model the possible leakage of fluid into the porous vertebrae. We therefore assume that the flux of liquid through each plate is proportional to the difference between the liquid pressure  $p_\ell$  and the external ambient pressure  $p_a$ . It follows that

$$\mathbf{n} \cdot (\mathbf{q}_\ell - \mathbf{q}_s) = h(p_\ell - p_a), \quad (2.21)$$

where  $\mathbf{n}$  is the outward normal and  $h$  is a scalar parameter representing the permeability;  $h \rightarrow 0$  implies impermeability while  $h \rightarrow \infty$  if fluid may pass freely through the plate. In general  $h$  should be a function of  $x$  and  $y$ , since the vertebrae are known to be more permeable near the centre than at the edges. If the velocities are eliminated, (2.21) becomes a Robin boundary condition for the pressure:

$$k(\phi_0) \frac{\partial p_\ell}{\partial z} = -\mu_\ell h(p_\ell - p_a) \quad \text{on} \quad z = \pm a. \quad (2.22)$$

The outer surface, initially given by  $x^2 + y^2 = L^2$ ,  $-a \leq z \leq a$ , is denoted by  $S$ . It is assumed to be open to fluid at uniform pressure  $p_a$ , so that

$$-(1 - \phi)(p_s - p_a)\mathbf{n} + \boldsymbol{\tau} \cdot \mathbf{n} = -(1 - \phi)(p_\ell + \pi - p_a)\mathbf{n} + \boldsymbol{\tau} \cdot \mathbf{n} = \mathbf{0}, \quad \mathbf{x} \in S, \quad (2.23)$$

where the outward-pointing normal is here given by  $\mathbf{n} = (x/\sqrt{x^2 + y^2}, y/\sqrt{x^2 + y^2}, 0)^T$ . As for the upper and lower plates,  $S$  is assumed to be semi-permeable to fluid, with permeability  $\eta$ , and this gives rise to a Robin condition of the form

$$k(\phi_0)\mathbf{n} \cdot \nabla p_\ell = -\mu_\ell \eta(p_\ell - p_a), \quad \mathbf{x} \in S. \quad (2.24)$$

In principle, (2.20–2.24) provide enough boundary conditions to solve (2.16–2.18) for  $\tilde{\phi}$ ,  $p_\ell$  and  $\mathbf{u}$ . The first-order motion of the free boundary is then found by evaluating the displacement  $\mathbf{u}$  at  $S$ . We can also use (2.5), (2.11), (2.6), *etc.* to calculate the elastic stress, fluid velocity and all other quantities of interest.

Initially, we assume that the porosity takes its undisturbed value and therefore

$$\tilde{\phi} = 0 \quad \text{when} \quad t = 0. \quad (2.25)$$

We are not at liberty to specify initial conditions for  $p_\ell$  or  $\mathbf{u}$ , both of which satisfy elliptic boundary-value problems. It might be anticipated that the disc should start at equilibrium with  $p_s = p_\ell = 0$ . Because of the additional osmotic pressure  $\pi$  in (2.23), however, the displacement field  $\mathbf{u}$  will not in general be zero initially. For the moment, we avoid this difficulty by assuming that the osmotic pressure is zero when the disc is in equilibrium, *i.e.* that  $\pi(\phi_0) = 0$ . Otherwise, it is nontrivial to determine the elastic stress in the disc even if no displacement is applied to the top and bottom, a problem that warrants further investigation.

## 2.3 Lubrication solution in two dimensions

### 2.3.1 Lubrication scaling

The simplifications we have employed thus far have enabled us to reduce the model to a linear boundary-value problem on a known, fixed domain. Further progress with the system (2.16–2.18) would require a numerical scheme to be devised, albeit of a fairly standard type. Instead, we reduce the model further by making use of the fact that the aspect ratio of a disc is typically rather large, around 5:1, which enables us to adopt a “lubrication” approximation. To simplify things as much as possible, we also restrict our attention to two dimensions, which allows us to investigate more easily “wedging” of the disc by twisting of the vertebral bodies. Our aim here is to gain some insight into the qualitative behaviour to be expected; in any case, there is little hope of our greatly simplified model producing any trustworthy quantitative information.

The disc now occupies the region  $-L \leq x \leq L$ ,  $-a \leq z \leq a$  in terms of the two-dimensional Cartesian coordinates  $(x, z)$ . The inverse aspect ratio, or slenderness parameter, is defined to be

$$\epsilon = \frac{a}{L},$$

and the lubrication approximation is obtained by taking the limit  $\epsilon \rightarrow 0$ . We use  $W_0$  as a representative value of the applied displacement  $W$  and nondimensionalise the equations and boundary conditions as follows:

$$\begin{aligned} x &= L\hat{x}, & z &= a\hat{z}, & W &= W_0\widehat{W}, & w &= W_0\widehat{w}, \\ u &= \frac{W_0}{\epsilon}\widehat{u}, & t &= \frac{a^2}{D}\widehat{t}, & \tilde{\phi} &= (1 - \phi_0)\frac{W_0}{a}\theta, & p_\ell &= p_a + \frac{\mu_\ell DW_0 L^2}{\phi_0 k(\phi_0) a^3} \widehat{p}, \end{aligned}$$

where  $\mathbf{u} = (u, w)^T$  is the two-dimensional displacement field. With the hats now dropped for ease of notation, (2.17) and (2.18) become

$$\epsilon^2 \frac{\partial}{\partial t} \left( \frac{\partial u}{\partial x} + \frac{\partial w}{\partial z} \right) = \epsilon^2 \frac{\partial^2 p}{\partial x^2} + \frac{\partial^2 p}{\partial z^2}, \quad (2.26)$$

$$\frac{\partial p}{\partial x} = \epsilon^2 A \frac{\partial}{\partial x} \left( \frac{\partial u}{\partial x} + \frac{\partial w}{\partial z} \right) + (1 - A) \left( \epsilon^2 \frac{\partial^2 u}{\partial x^2} + \frac{\partial^2 u}{\partial z^2} \right), \quad (2.27)$$

$$\frac{\partial p}{\partial z} = \epsilon^2 A \frac{\partial}{\partial z} \left( \frac{\partial u}{\partial x} + \frac{\partial w}{\partial z} \right) + \epsilon^2 (1 - A) \left( \epsilon^2 \frac{\partial^2 w}{\partial x^2} + \frac{\partial^2 w}{\partial z^2} \right), \quad (2.28)$$

where

$$A = \frac{\lambda + \mu - (1 - \phi_0)^2 \pi'(\phi_0)}{\lambda + 2\mu - (1 - \phi_0)^2 \pi'(\phi_0)} \in (0, 1).$$

The porosity perturbation is determined *a posteriori* from

$$\theta = \frac{\partial u}{\partial x} + \frac{\partial w}{\partial z}. \quad (2.29)$$

The boundary conditions are

$$u = 0, \quad w = \pm W(x, t), \quad \frac{\partial p}{\partial z} = \mp \epsilon^2 H(x)p \quad \text{at } z = \pm 1 \text{ for } -1 \leq x \leq 1, \quad (2.30)$$

$$\frac{\partial u}{\partial x} + \frac{2\mu}{\lambda + 2\mu} \frac{\partial w}{\partial z} = 0, \quad \frac{\partial u}{\partial z} + \epsilon^2 \frac{\partial w}{\partial x} = 0, \quad \frac{\partial p}{\partial x} = \mp Y(z)p \quad \text{at } x = \pm 1 \text{ for } -1 \leq z \leq 1, \quad (2.31)$$

where

$$H(x) = \left( \frac{L^2 \mu_\ell}{ak(\phi_0)} \right) h(x), \quad Y(z) = \left( \frac{L\mu_\ell}{k(\phi_0)} \right) \eta(z).$$

Recall that  $h$  and  $\eta$  are the dimensional permeabilities of the horizontal and vertical surfaces of the disc, respectively, and therefore need not be equal. As we shall see, the richest asymptotic limit is obtained by assuming they are such that  $H$  and  $Y$  are both  $O(1)$  as  $\epsilon \rightarrow 0$ .

### 2.3.2 Leading-order equations

We expand the dependent variables as follows:

$$p \sim p_0 + \epsilon^2 p_1 + \dots, \quad u \sim u_0 + \epsilon^2 u_1 + \dots, \quad w \sim w_0 + \epsilon^2 w_1 + \dots$$

At leading order, (2.28) shows that

$$p_0 = p_0(x, t),$$

so that (2.26) is satisfied automatically at leading order. Equation (2.27) then gives us

$$(1 - A) \frac{\partial^2 u_0}{\partial z^2} = \frac{\partial p_0}{\partial x}$$

and hence

$$u_0 = \frac{z^2 - 1}{2(1 - A)} \frac{\partial p_0}{\partial x} \quad (2.32)$$

is the solution that satisfies  $u_0 = 0$  at  $z = \pm 1$ .

At  $O(\epsilon^2)$ , (2.28) shows that

$$\frac{\partial p_1}{\partial z} = A \frac{\partial^2 u_0}{\partial x \partial z} + \frac{\partial^2 w_0}{\partial z^2} = \frac{Az}{1 - A} \frac{\partial^2 p_0}{\partial x^2} + \frac{\partial^2 w_0}{\partial z^2}, \quad (2.33)$$



while (2.26) gives

$$\frac{\partial}{\partial t} \left( \frac{\partial u_0}{\partial x} + \frac{\partial w_0}{\partial z} \right) = \frac{\partial^2 p_0}{\partial x^2} + \frac{\partial^2 p_1}{\partial z^2}$$

and hence, from (2.33),

$$\begin{aligned} \frac{\partial}{\partial t} \left\{ \frac{z^2 - 1}{2(1-A)} \frac{\partial^2 p_0}{\partial x^2} + \frac{\partial w_0}{\partial z} \right\} &= \frac{1}{1-A} \frac{\partial^2 p_0}{\partial x^2} + \frac{\partial^3 w_0}{\partial z^3} \\ &= \frac{\partial^2}{\partial z^2} \left\{ \frac{z^2 - 1}{2(1-A)} \frac{\partial^2 p_0}{\partial x^2} + \frac{\partial w_0}{\partial z} \right\}. \end{aligned}$$

This is simply the leading-order version of the diffusion equation (2.19) for  $\tilde{\phi}$ . If we integrate with respect to  $z$  and use the fact that  $w_0$  is an odd function of  $z$  to eliminate the constant of integration, we arrive at

$$\frac{\partial \psi}{\partial t} = \frac{\partial^2 \psi}{\partial z^2}, \quad (2.34)$$

where

$$\psi = \frac{1}{2(1-A)} \left( \frac{z^3}{3} - z \right) \frac{\partial^2 p_0}{\partial x^2} + w_0. \quad (2.35)$$

At leading order, the boundary condition (2.30) becomes

$$\frac{\partial p_1}{\partial z} = \frac{A}{1-A} \frac{\partial^2 p_0}{\partial x^2} + \frac{\partial^2 w_0}{\partial z^2} = -H p_0 \quad \text{at } z = 1,$$

or, in terms of  $\psi$ ,

$$\frac{\partial^2 p_0}{\partial x^2} - H p_0 = \frac{\partial \psi}{\partial t} \Big|_{z=1}. \quad (2.36)$$

The boundary condition at  $z = -1$  is identical, by symmetry. We can also write the boundary condition on the vertical displacement,  $w_0 = W(x, t)$  at  $z = 1$ , in terms of  $\psi$ , to obtain

$$\frac{\partial^2 p_0}{\partial x^2} = 3(1-A) (W - \psi|_{z=1}). \quad (2.37)$$

Again, symmetry requires that an identical boundary condition be imposed on  $z = -1$ ; indeed, we can restrict our attention to the half-disc  $z > 0$  by setting

$$\psi = 0 \quad \text{at } z = 0. \quad (2.38)$$

To conclude, we have to solve the diffusion equation (2.34) for  $\psi$  with the boundary conditions (2.36, 2.37) on  $z = 1$  and (2.38) on  $z = 0$ . The initial condition for  $\psi$  is simply

$$\psi = 0 \quad \text{at } t = 0. \quad (2.39)$$

Notice that  $\psi$  satisfies a boundary-value problem in  $z$  and  $t$ , with  $x$  merely a parameter. On the other hand,  $p_0$  effectively satisfies an ordinary differential equation in  $x$ , depending only parametrically on  $t$ . The coupling of these through the boundary conditions (2.36) and (2.37) leads to a mathematically interesting, although rather tricky problem.

To complete the system, we also need the leading-order boundary conditions on  $p_0$  at the edges of the disc, namely

$$\frac{\partial p_0}{\partial x} = \mp Y p_0 \quad \text{at } x = \pm 1. \quad (2.40)$$

Note that this requires us to assume that  $Y$  is independent of  $z$ , which seems physiologically reasonable. Otherwise, there must be boundary layers near  $x = \pm 1$ , of thickness  $O(\epsilon)$ , over which  $z$ -variations in  $p_0$  decay. The stress-free boundary conditions (2.31*a, b*) must likewise be satisfied across edge layers; this structure is consistent with stress profiles like those shown in figure 1.

Once we have solved for  $\psi$  and the dimensionless fluid pressure  $p$ , the leading-order deviatoric stress components may be determined from (2.11):

$$\begin{aligned} \tau_{xx} &= \frac{W_0}{a} \left( (\lambda + 2\mu) \frac{\partial u}{\partial x} + \lambda \frac{\partial w}{\partial z} \right) \\ &\sim \frac{W_0}{a} \left( 2\mu \frac{z^2 - 1}{2(1-A)} \frac{\partial^2 p_0}{\partial x^2} + \lambda \frac{\partial \psi}{\partial z} \right) \end{aligned} \quad (2.41)$$

$$\begin{aligned} \tau_{xz} &= \frac{\mu W_0}{a} \left( \frac{\partial u}{\partial z} + \epsilon^2 \frac{\partial w}{\partial x} \right) \\ &\sim \frac{\mu W_0}{\epsilon a} \left( \frac{z}{1-A} \frac{\partial p_0}{\partial x} \right) \end{aligned} \quad (2.42)$$

$$\begin{aligned} \tau_{zz} &= \frac{W_0}{a} \left( \lambda \frac{\partial u}{\partial x} + (\lambda + 2\mu) \frac{\partial w}{\partial z} \right) \\ &\sim \frac{W_0}{a} \left( -2\mu \frac{z^2 - 1}{2(1-A)} \frac{\partial^2 p_0}{\partial x^2} + (\lambda + 2\mu) \frac{\partial \psi}{\partial z} \right). \end{aligned} \quad (2.43)$$

We may thus quantify the stress experienced by the elastic matrix of the disc, with the eventual aim of estimating the possible consequent damage and/or remodelling.

### 2.3.3 Simple solutions

The initial/boundary value problem given by (2.34) to (2.40) is difficult to solve in general. It may be reduced to an ordinary differential equation using Laplace transforms, but this isn't really much help. For the purposes of this report, we consider a few simple scenarios for which exact solutions exist. To begin with, suppose that  $H$  is constant and we seek a time-harmonic solution with  $W = e^{i\omega t}$ . It is straightforward, without solving the diffusion equation for  $\psi$ , to show that

$$p_0 = i\omega \left( \frac{\cosh kx}{k \sinh k + \cosh k} - \frac{1}{Y} \right) e^{i\omega t},$$

where

$$k^2 = \frac{3(1-A)H}{3(1-A) + i\omega}.$$

It is then straightforward to find the long-time solution for  $\psi$  in the form

$$\psi = \left( \frac{Y(k^2 - H) \cosh kx}{H(k \sinh k + \cosh k)} + H \right) \frac{\sinh z \sqrt{i\omega}}{\sinh \sqrt{i\omega}} e^{i\omega t}. \quad (2.44)$$

Similarly, if the upper and lower surfaces are impermeable, with  $H = 0$ , we have

$$\left. \frac{\partial \psi}{\partial t} \right|_{y=1} + 3(1-A) \psi|_{y=1} = 3(1-A)W,$$

which can be solved independently of the diffusion problem. Suppose we consider the case where the disc is uniformly squeezed, so that  $W = -1$  say. Again, it is easy to obtain the pressure, which reads

$$p_0 = \frac{3}{2}(1-A)e^{-3(1-A)t} \left( 1 + \frac{2}{Y} - x^2 \right).$$

The pressure obtained in this case is akin to that shown in figure 1(a), albeit without the flat centre. We solve for  $\psi$  to find that

$$\psi = \frac{\sin \sqrt{3(1-A)}z}{\sin \sqrt{3(1-A)}} e^{-3(1-A)t} - z + \sum \frac{4}{n\pi} \left[ \frac{n\pi - \sin n\pi}{2n\pi - \sin 2n\pi} \right] e^{-n^2\pi^2 t} \sin n\pi(1-z), \quad (2.45)$$

provided  $A \neq m^2\pi^2/3$  (which can never happen since  $0 \leq A \leq 1$ ). We can then solve for  $\theta$  using

$$\theta = \frac{\partial \psi}{\partial z} = \left( \sqrt{3(1-A)} e^{-3(1-A)t} \frac{\cos \sqrt{3(1-A)}z}{\sin \sqrt{3(1-A)}} - 1 - 4 \sum \left[ \frac{n\pi - \sin n\pi}{2n\pi - \sin 2n\pi} \right] e^{-n^2\pi^2 t} \cos n\pi(1-z) \right),$$

and we can readily see that  $\theta \rightarrow -1$  as  $t \rightarrow \infty$ , indicating that the liquid volume fraction decreases as the disc is compressed. We can also use the solutions for  $p_0$  and  $\psi$  to find the stress components in the disc;

$$\begin{aligned} \tau_{xx} \sim & \frac{W_0}{a} \left( -3\mu(z^2 - 1)e^{-3(1-A)t} + \lambda \left( \sqrt{3(1-A)} e^{-3(1-A)t} \frac{\cos \sqrt{3(1-A)}z}{\sin \sqrt{3(1-A)}} \right. \right. \\ & \left. \left. - 1 - 4 \sum \left[ \frac{n\pi - \sin n\pi}{2n\pi - \sin 2n\pi} \right] e^{-n^2\pi^2 t} \cos n\pi(1-z) \right) \right), \end{aligned} \quad (2.46)$$

$$\tau_{xz} \sim -3 \frac{\mu W_0}{\epsilon a} x z e^{-3(1-A)t}, \quad (2.47)$$

$$\begin{aligned} \tau_{zz} \sim & \frac{W_0}{a} \left( 3\mu(z^2 - 1)e^{-3(1-A)t} + (\lambda + 2\mu) \left( \sqrt{3(1-A)} e^{-3(1-A)t} \frac{\cos \sqrt{3(1-A)}z}{\sin \sqrt{3(1-A)}} \right. \right. \\ & \left. \left. - 1 - 4 \sum \left[ \frac{n\pi - \sin n\pi}{2n\pi - \sin 2n\pi} \right] e^{-n^2\pi^2 t} \cos n\pi(1-z) \right) \right). \end{aligned} \quad (2.48)$$

Note that the long time behaviour is that the stress components are constant;  $\tau_{xx} \rightarrow -W_0\lambda/a$ ,  $\tau_{xz} \rightarrow 0$  and  $\tau_{zz} \rightarrow -W_0(\lambda + 2\mu)/a$  as  $t \rightarrow \infty$ . The anticipated qualitative behaviour, whereby the fluid pressure decays at large times and the elastic stress takes up the load, is thus reproduced.

Finally, we consider the situation in which the discs are deformed, so that they converge as  $x$  increases. We set  $w = -x$ , and find that the pressure is given by

$$p_0 = \frac{(1-A)}{2} e^{-3(1-A)t} x \left\{ \frac{Y+3}{(1+Y)} - x^2 \right\}.$$

The solution for  $\psi$  in this case is given by  $x$  times the solution given in (2.45) and, therefore  $\theta \rightarrow -x$  as  $t \rightarrow \infty$ . Thus the volume fraction of the liquid phase decreases linearly from the centre to the compressed edge of the disc.

We calculate that the components of the stress in the disc in this case are

$$\begin{aligned} \tau_{xx} \sim & \frac{W_0}{a} \left( -3\mu(z^2 - 1)xe^{-3(1-A)t} + \lambda x \left( \sqrt{3(1-A)}e^{-3(1-A)t} \frac{\cos \sqrt{3(1-A)}z}{\sin \sqrt{3(1-A)}} \right. \right. \\ & \left. \left. - 1 - 4 \sum \left[ \frac{n\pi - \sin n\pi}{2n\pi - \sin 2n\pi} \right] e^{-n^2\pi^2 t} \cos n\pi(1-z) \right) \right), \end{aligned} \quad (2.49)$$

$$\tau_{xz} \sim \frac{\mu W_0}{2\epsilon a} z e^{-3(1-A)t} \left( \frac{3+Y}{1+Y} - 3x^2 \right), \quad (2.50)$$

$$\begin{aligned} \tau_{zz} \sim & \frac{W_0}{a} \left( 3\mu(z^2 - 1)xe^{-3(1-A)t} + (\lambda + 2\mu)x \left( \sqrt{3(1-A)}e^{-3(1-A)t} \frac{\cos \sqrt{3(1-A)}z}{\sin \sqrt{3(1-A)}} \right. \right. \\ & \left. \left. - 1 - 4 \sum \left[ \frac{n\pi - \sin n\pi}{2n\pi - \sin 2n\pi} \right] e^{-n^2\pi^2 t} \cos n\pi(1-z) \right) \right). \end{aligned} \quad (2.51)$$

Note that the long-time behaviour of the stress components in this case are  $\tau_{xx} \rightarrow -\lambda W_0 x/a$ ,  $\tau_{xz} \rightarrow 0$  and  $\tau_{zz} \rightarrow -W_0(\lambda + 2\mu)x/a$  as  $t \rightarrow \infty$ . At large times, the stress is nonuniform across the disc, in contrast with a uniform hydrostatic pressure.

## 2.4 Conclusions

In this report we have developed a mathematical model describing the deformation of an intervertebral disc under an applied load. We have modelled the disc as a poroelastic matrix that is saturated with a viscous liquid. We model the presence of the proteoglycans as a pressure difference between the two phases. We imposed conservation of mass and momentum to the two phases (namely matrix and fluid). We reduced the stated model to three coupled equations for the matrix velocity, the volume fraction of the fluid, and the pressure in the fluid phase. We simplified the model by assuming that the deformations of the matrix are governed by linear-elasticity theory. We then utilised the slenderness of the disc to further reduce the model. We solved the simplified model for several prescribed displacements of the free surface.

The model is a first step towards describing the behaviour of an intervertebral disc. There are numerous extensions to this preliminary investigation that could be undertaken.

- Firstly, the coupled problem for  $\psi$  and  $p_0$  (equation (2.34) and the associated boundary conditions) could be solved for a physically realistic (spatially varying) permeability.
- Secondly, the thin-disc analysis should be extended to the naturally more realistic circular geometry.
- Thirdly, the non-slender version of the model could be solved numerically.
- Finally, we should enhance the model to include the effects of changing the parameters over time, so that we can assess whether or not remodelling acts to enhance any initial asymmetry in the system.

## References

- [1] Fitt, A.D., Howell, P.D., King, J.R., Please, C.P. & Schwendeman, D.W. (2002) Poroelastic multi-phase flow modelling for paper squeezing. *Euro. J. Appl. Maths*, to appear.